Isotope Effects in the Formation of Molecular Hydrogen on a Graphite Surface via an Eley−Rideal Mechanism

Anthony J. H. M. Meijer,* Adam J. Farebrother, and David C. Clary†

Department of Chemistry, University College London, 20 Gordon Street, London, WC1H 0AJ United Kingdom

Received: April 17, 2002; In Final Form: June 27, 2002

The associative desorption of HD (v,j) and D_2 (v,j) on a graphite(0001) surface via an Eley−Rideal mechanism has been studied theoretically using a time-dependent wave packet method. We find that product molecules are formed rovibrationally excited and translationally hot. When comparing the different products to earlier calculations on the formation of H_2 on graphite(0001), we find significant isotope effects and possible resonant transitions during the reaction, which might have consequences for the possible detection of highly excited H_2 in dense intermolecular clouds.

1. Introduction

The current paper is a continuation of previous theoretical studies on the formation of H_2 by associative desorption on a graphite surface.[1,2] Associative desorption is the reverse reaction from dissociative adsorption, a process that has been studied extensively, both experimentally (see, e.g., refs 3−6) and theoretically (see, e.g., refs 7−14).

Generally speaking, there are two distinct mechanisms through which associative desorption can occur, the Langmuir−Hinshelwood mechanism and the Eley−Rideal mechanism.[15] In the Langmuir−Hinshelwood mechanism both particles involved in the reaction are initially adsorbed on the surface and thermalized to it. Subsequently, these particles move across the surface by tunneling or by diffusion. Upon encountering each other they react and desorb. The energy released will be partly absorbed by the surface and partly taken away by the product molecule. In the (direct) Eley−Rideal mechanism only one particle is adsorbed on the surface and thermalized to it. The second particle collides with the first particle without first thermalizing to the surface, forming a molecule that desorbs. In the Eley−Rideal mechanism more excess energy will be available to the product, because only one bond with the surface has to be broken.

The Langmuir−Hinshelwood mechanism has been studied more extensively than the Eley−Rideal mechanism, because of its importance in catalysis. However, in recent years, reactions in which the Eley−Rideal mechanism plays an important role have also been found.[4,16−23] Theoretically, most research has been done on catalytic systems,[24−30] although some astrophysically relevant systems have also been studied.[1,2,31−35]

The primary motivation for studying the formation of H_2 and its isotopic analogues on graphite lies in astrophysics. The hydrogen molecule is the most abundant in space, especially in dense molecular clouds. Its formation mechanism has been a subject of much debate in the past. However, currently, the generally accepted mechanism for the formation of H_2 is via associative desorption on interstellar dust grains.[36−39] This mechanism is the only one proposed that can explain the abundance of H_2 in the interstellar medium. Note that the nature of these interstellar dust grains is not precisely known. However, there is evidence from the analysis of meteorites that dust may be coated in carbon.[40−42] Other evidence is available as well.[43−45] Therefore, most models include amorphous carbon.[46] In our calculations we use graphite(0001) as a model for interstellar grains.

In previous papers we studied the formation of H_2 on graphite.[1,2] We concluded from our calculations that H_2 formed in highly excited rovibrational states. This has important consequences for reactions in the interstellar medium, because the excess energy can be used to overcome reaction barriers in endothermic reactions. We also find that H_2 is formed translationally hot, which can lead to localized heating of molecular clouds due to inelastic collisions.

In this paper, as in our previous papers,[1,2] we only study the formation of H_2. The formation of the H−graphite system is not considered in our calculations but is taken as an initial condition. The precise structure of this system, i.e., whether H will be physisorbed or chemisorbed on the graphite surface, has been the subject of some discussion recently. Experiments on the formation of HD on graphite surfaces show that H and D can be physisorbed on the surface with a very low mobility across the surface.[47−49] In a different experiment the physisorption well depth was measured to be 43 ± 0.5 meV.[50] In DFT calculations Sha and Jackson find a well depth of 7.75 meV for the physisorption well with a barrier to chemisorption of 0.2 eV and essentially no barrier to diffusion across the surface.[32] This value compares well to an earlier calculation by Sidis et al.,[51] who found a value of 8 meV. Our own calculations show a physisorption well and barrier to chemisorption as well (See Figure 2 of ref 2). However, the number of DFT points in the area is not large enough to give us an accurate estimate of the barrier height and of the physisorption well depth. The barrier of 0.2 eV found by Sha and Jackson would make it unlikely that an H atom will chemisorb on a bare graphite surface. However, we wish to point out here that DFT is generally not considered to describe physisorption processes well, because they are dominated by dispersion interactions. Note that the possible barrier to chemisorption on a graphite surface does not mean that chemisorption of H will not occur on interstellar dust, because interstellar dust will not be pure graphite and because

* Corresponding author. E-mail: a.meijer@ucl.ac.uk.
† E-mail: d.c.clary@ucl.ac.uk.

10.1021/jp020983h CCC: $22.00
Published on Web 09/04/2002

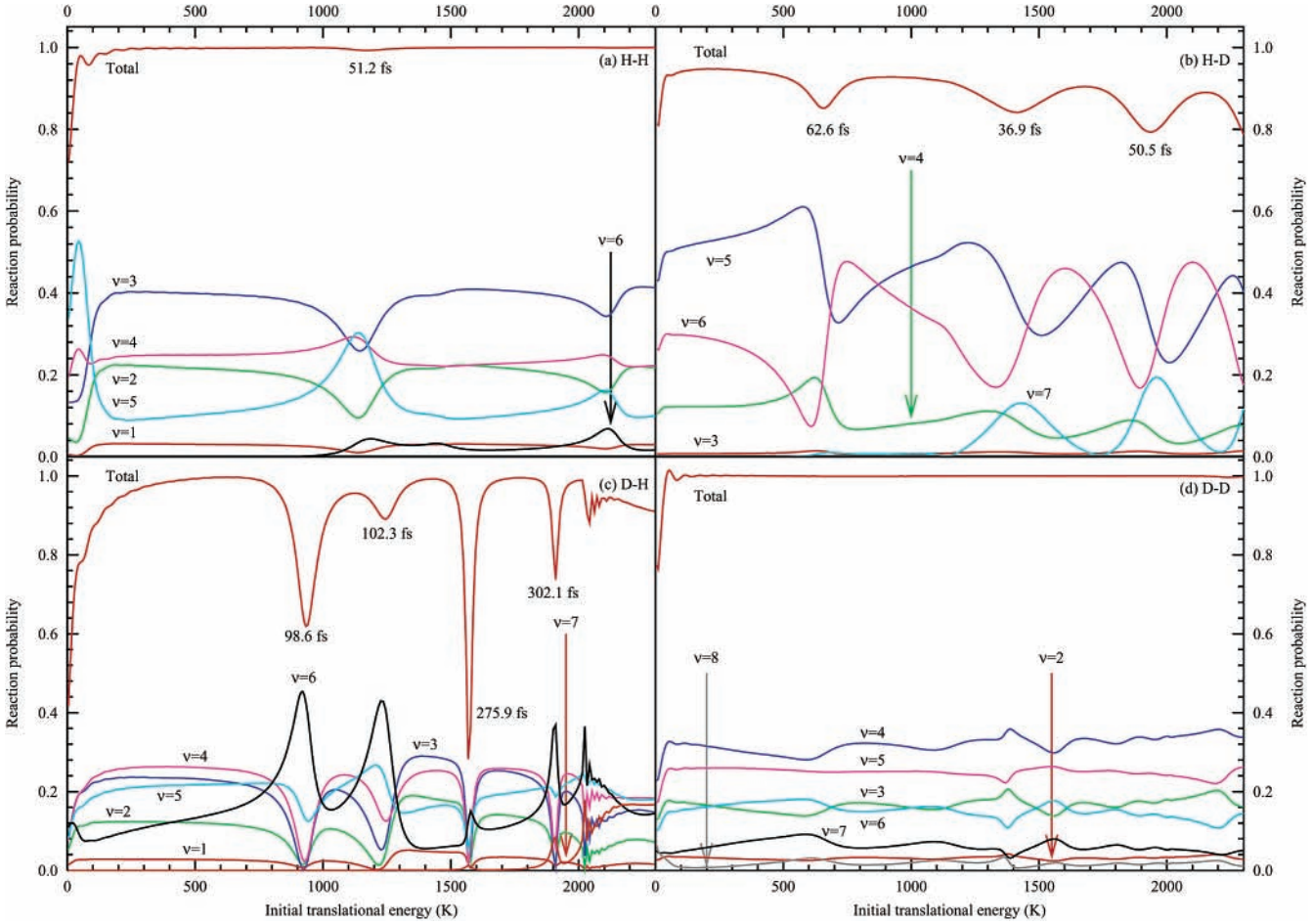

Figure 1. 2D reaction probabilities for the H−H, H−D, D−H, and D−D reactions.

other molecules will be adsorbed on the dust as well, which will significantly change the potential energy surface (PES).

Our dynamics results can be compared with other studies on the surface-catalyzed formation of H_2 on graphite, which have appeared in the literature since our previous calculations. Sha and Jackson[32,52] recently reported on quantum mechanical calculations on a new ab initio density functional theory (DFT) surface in which they also included the influence of subsurface carbon atoms. Their potential shows a comparable exothermicity for the formation of H_2, comparable H−graphite chemisorption energy, and a similar fast decrease of the PES, once the formed H_2 leaves the frozen surface. Also, they find that their PES has a small barrier, whereby it should be noted that a method such as DFT is not expected to give highly accurate reaction barriers for such a system. As a result they find that reaction probabilities decrease with decreasing temperature. For energies of astrophysical interest they find H_2 with an average vibrational quantum number, $\langle v \rangle$, of approximately 6 and an average rotational quantum number, $\langle j \rangle$, of 2.[32] In quantum mechanical calculations based on earlier DFT calculations by Jeloaica and Sidis,[53] Jackson and Lemoine[31] found that H_2 is formed with $\langle v \rangle = 8-9$ and $\langle j \rangle = 5-6$. Using a potential based on the same DFT calculations, Rutigliano, Cacciatore, and Billing[34] find in their semiclassical calculations, which include phonon motion, that H_2 is formed rovibrationally excited ($v = 3-6$ and $j = 8-11$) with a maximum rotational quantum number j of 22. Finally, in classical trajectory calculations including a model for the surface phonons, Ree, Kim, and Shin[35] find that H_2 is formed vibrationally excited with a maximum at $v = 3$ and still significant excitation in $v = 8-10$. We wish to emphasize here that all calculations discussed here make approximations in the potential and its fitting as well as in the description of the dynamics of the reaction. This will obviously influence the results.

In the current paper we discuss the formation of HD and D_2 on a graphite surface via the Eley−Rideal mechanism. The motivation for this is to investigate the influence of changing the mass combinations of the particles involved on the reaction probabilities. Also, we use the isotope-substituted reactions as a way to get a better insight into the precise reaction dynamics of the H_2 reaction. Thus, we have calculated the probabilities of producing HD and D_2 in specific rovibrational states as a function of initial translational energy using a time-dependent wave packet formalism. We investigated the formation of HD both from the situation in which H was initially adsorbed as well as from the situation in which D was initially adsorbed. For our calculations we used the same potential as in ref 1.

The paper is organized as follows. In sections 2 and 3 we discuss the theory and some computational details. In section 4 we discuss our results, and in section 5 we discuss our conclusions.

2. Theory

Most of the theory used in this paper has been published before.[1] Therefore, we will just highlight some important details and refer the reader for a more in-depth discussion to ref 1.

2.1. Coordinate System and Potential. We start by introducing our notation. The Cartesian coordinates of the incident atom are given as $\mathbf{x}_i = (x_i, y_i, z_i)$, whereas those of the target atom are given as $\mathbf{x}_t = (x_t, y_t, z_t)$. However, we find it more convenient to use Jacobi coordinates in our calculations. Thus,

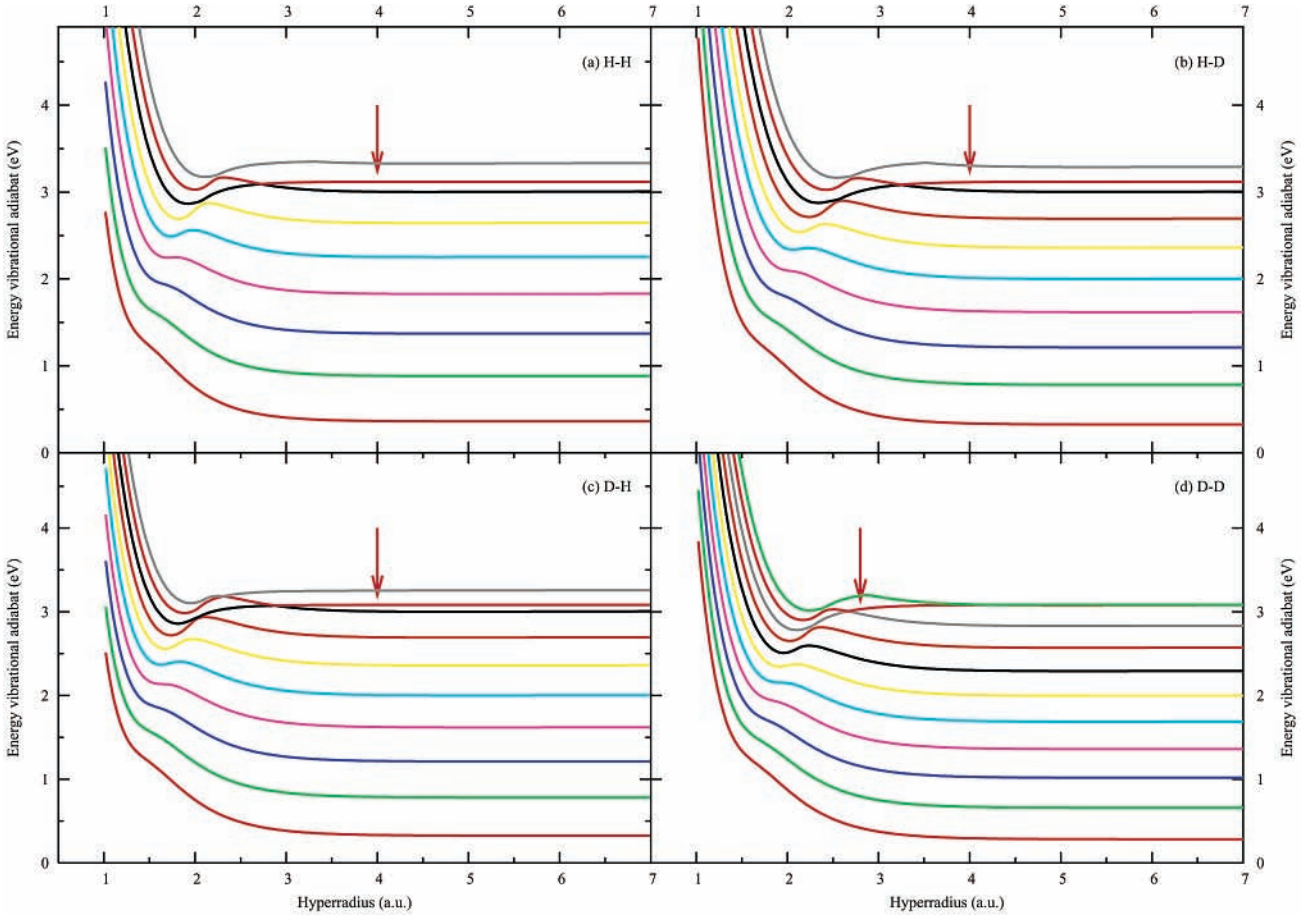

Figure 2. Vibrational adiabatic curves as a function of the hyperradius for the H−H, H−D, D−H, and D−D reactions. The arrow indicates the vibrational adiabat followed in the time-independent scattering calculations.

we use the relative position vector $\mathbf{r} = \mathbf{x}_t - \mathbf{x}_i$ and the center-of-mass position vector $\mathbf{X} = (m_i\mathbf{x}_i + m_t\mathbf{x}_t)/(m_i + m_t)$, where m_i and m_t are the masses of the incident and target atoms, respectively. $\mathbf{r}$ is most conveniently expressed in polar coordinates $\mathbf{r} = (r, \vartheta, \varphi)$, where r is the length of $\mathbf{r}$ and ϑ and φ are the polar and azimuthal angles, respectively. $\mathbf{X}$ is used in Cartesian coordinates $\mathbf{X} = (X, Y, Z)$, where X, Y, and Z indicate the position of the center-of-mass of the molecule above the surface.

In our calculations we use the fixed, flat surface approximation. This means that we neglect the influence of both surface phonons and corrugation on the reaction probabilities. This approximation implies that no energy transfer will occur between the forming H_2 molecule and the solid. This should be a reasonable approximation for the dynamics of this system, because of the mass difference between H/D and C. Also, Ruttigliano and co-workers have shown[34] in a calculation in which the phonons were included (classically) that energy transfer to the solid should be around 0.1 eV independent of the temperature of the solid, making the energy transfer a small percentage of the available exothermicity. The fixed, flat surface approximation has been used extensively and successfully in the past.[1,24−26,31,54] It allows the dynamics to become independent of ϕ, X, and Y. Thus, the potential V depends only on Z, r, and ϑ, reducing the six-dimensional calculation to a three-dimensional one. The basis functions in Z and r, like in ref 1, are "wrapped" sinc-DVR (discrete variable representation) functions.[55−58] We use a Gauss−Legendre DVR basis in ϑ.[59,60] This basis is symmetry-adapted in the case of the formation of H_2 and D_2,[61,62] allowing us to perform calculations for odd and even rotational states separately.

Our potential is of the LEPS (London−Eyring−Polyani−Sato) form, adapted for use with surfaces.[63] It is an eight-parameter interaction potential, based on earlier DFT calculations.[1,2] Its complete form is given in ref 1. This potential is used here (rather than, e.g., the potential by Sha and Jackson[32]), so we can report on a thorough study of isotope effects by comparing with the previous results on the formation of H_2.

2.2. Hamiltonian, Propagation, Final Analysis, and Initial State. With our current choice of the coordinate system, the Hamiltonian is written as

$$\hat{H} = -\frac{\hbar^2}{2M}\frac{\partial^2}{\partial Z^2} - \frac{\hbar^2}{2\mu}\frac{\partial^2}{\partial r^2} + \frac{\hat{J}^2}{2\mu r^2} + V(Z,r,\vartheta) \qquad (1)$$

where M and μ are the total mass and the reduced mass of the product molecule, respectively. This Hamiltonian is equal to the one commonly used to study dissociative adsorption, when the surface is assumed to be flat and fixed. The equations-of-motion corresponding to the Hamiltonian in eq 1 and the current choice of the basis are given in ref 1.

The wave function is propagated in time using the real wave packet method of Gray and Balint-Kurti.[64−67] In this method reaction probabilities are calculated from only the real part q of the wave packet Ψ. q is propagated in time using a modified Schrödinger equation where $\hat{H}$ is replaced by a function of itself, $f(\hat{H})$. For a judicious choice of $f(\hat{H})$, the propagation is given by a Chebychev recursion relation:

$$q_{\kappa+1} = \mathbf{A}(-\mathbf{A}q_{\kappa-1} + 2\mathbf{H}_s q_\kappa) \qquad (2)$$

where $\mathbf{H}_s = a_s\mathbf{H} + b_s$. a_s and b_s are chosen in such a way the

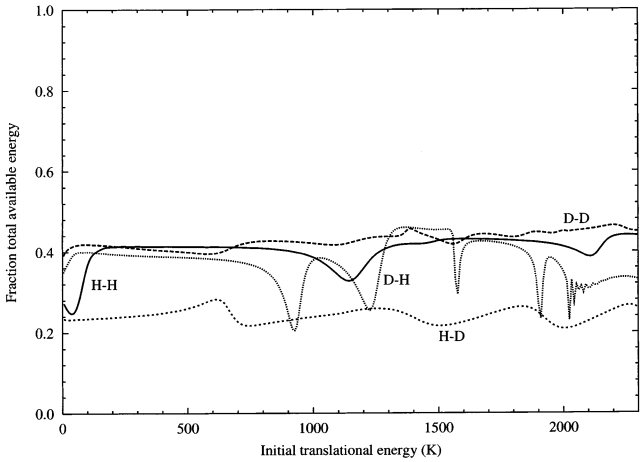

Figure 3. Average final translational energy as a percentage of the total energy available to the system for the four mass combinations for the 2D calculations.

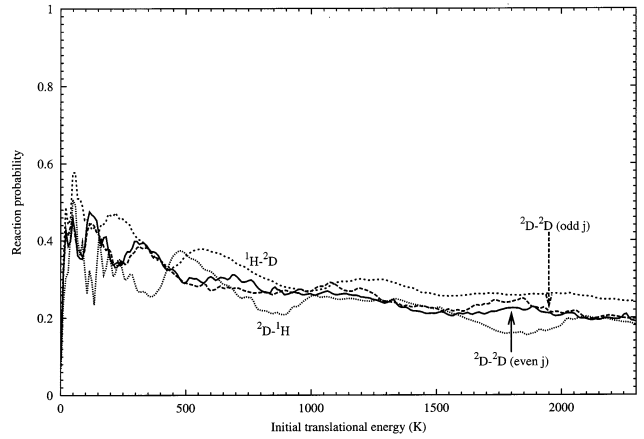

Figure 4. 3D total reaction probabilities for the H−H, H−D, D−H, and D−D reactions.

eigenvalues of $\mathbf{H}_s$ lie between −1 and +1, whereby $\mathbf{H}$ is the matrix representation of $\hat{H}$. The wave packet is adsorbed at the edges by the damping matrix $\mathbf{A}$ to avoid unphysical reflections.[68]

The final analysis is performed using a flux-based method.[65,69,70] In this method the total reaction probability, $P_r(E)$, is calculated from the energy-dependent flux through a surface in the exit channel at $Z_s = 10$ bohr. The state-resolved reaction probability, $P_{vj}(E)$, is calculated by projecting the energy-dependent wave functions used in the calculation of $P_r(E)$ onto the rovibrational energy functions of the H_2 molecule, which are labeled by the vibrational quantum number v and the rotational quantum number j. In this paper we only deal with collisions that are initially perpendicular to the surface. Therefore, the azimuthal rotational quantum number, m, equals zero. For more details, see refs 65, 69, and 70.

In both the 2D and the 3D calculations we calculate line widths and lifetimes for resonances in the total reaction probabilities by fitting sharp peaks in the total reaction probability to the Breit−Wigner function

$$P_r(E) = \frac{a}{(E - E_r)^2 + \frac{1}{4}\Gamma^2} \qquad (3)$$

where the fit constants a, E_r, and Γ are the strength of the resonance, the resonance energy, and the resonance line width, respectively. From Γ we can calculate the resonance lifetime τ through the energy−time uncertainty principle, i.e., $\tau = \hbar/\Gamma$. We only calculate the resonance lifetimes in cases where the resonance is well separated from other resonances, because eq 3 is not well suited if two resonances overlap. This fitting procedure to obtain lifetimes has been used successfully in gas-phase scattering calculations (see, e.g., refs 71 and 72).

The initial wave function is generated as a function of z_i and z_t, the heights of the incident and target atoms, respectively, and the impact parameter b as

$$\mathscr{Y}^{m=0}(z_i,z_t,b) = \frac{1}{\sqrt[4]{2\pi\beta}} e^{-ik_0 z_i} e^{-(z_i - z_0)^2/4\beta} v_0(z_t)\, F(b) \qquad (4)$$

Here, $v_0(z_t)$ is the vibrational ground state of the atom adsorbed on the surface. k_0 is the initial linear momentum of the incident atom and z_0 is the initial center of the wave packet. The initial distribution in b, $F(b)$, is given as

$$F(b) = \frac{2\pi}{A_b}\begin{cases} 1 & b < b_{max} \\ e^{-[(b-b_{max})\gamma]^2} & b > b_{max} \end{cases} \qquad (5)$$

where A_b is the normalization constant of $F(b)$. After $\mathscr{Y}^{m=0}(z_i,z_t,b)$ is generated, the initial wave function is trivially transformed to the (Z, r, ϑ) coordinates.[1,64] Note that $F(b)$ is not an eigenstate of the radial Hamiltonian. Therefore, it is possible for the final solution to depend on z_0, because of spreading and distortion of the wave packet. We removed this difficulty by making the initial wave packet quite diffuse, choosing $\gamma = 0.2$ bohr^{-1}, $b_{max} = 5$ bohr, and $z_0 = 14$ bohr.

3. Computational Details

Most parameters used in our calculations are similar to the ones used in our time-dependent study on the formation of H_2.[1] We used a slightly different approach from the previous paper[1] in that for the 2D calculations we use two different wave packets. The first wave packet is broad and has very low translational energy. The second wave packet is narrow with a relatively high initial translational energy. For the 3D calculations we found that at low translational energy the results from the high-energy wave packet and the low-energy wave packet were identical. Therefore, our results for the 3D calculations are only based on the narrow wave packets with high initial translational energy. The consequence of this strategy is that the reaction probabilities have been calculated for much higher energies than reported on here. We will only report reaction probabilities for the same energy range as in ref 1 for comparison purposes and reserve the other results for a later publication. The use of a higher energy wave packet did mean that for the calculations on HD and D_2 we had to increase the number of DVR points in the Z coordinate to 250 and 300, respectively and the number of DVR points in the r coordinates to 350 and 450, respectively. Note that for the 3D calculations in the case of deuterium colliding with deuterium adsorbed on graphite and of hydrogen colliding with adsorbed hydrogen, we can perform calculations for the odd and even rotational states of the resultant H_2 or D_2 molecules separately, effectively halving the size of the calculation. For H colliding with adsorbed D and for D colliding with adsorbed H all rotational states have to be included in one calculation.

The implementation of the various algorithms was also mostly identical to ref 1, apart from some optimizations. We still use the sorting algorithm by Groenenboom and Colbert[56] and the point selection algorithm by Meijer and Goldfield.[70] However, instead of running the computer code on a single processor of a 48 processor Origin 2000 at the Hiperspace Center at

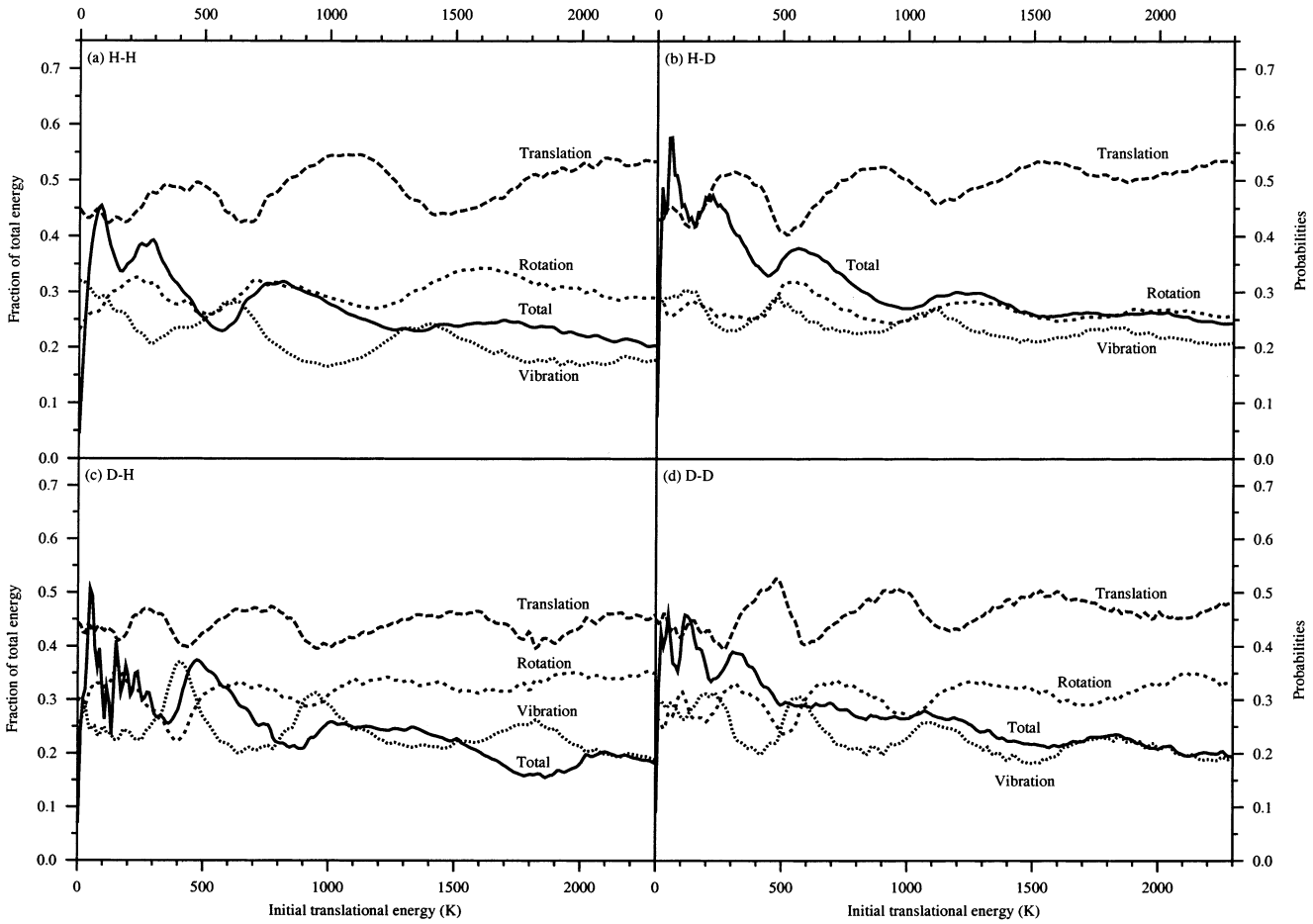

Figure 5. 3D reaction probabilities (total) and percentage of total energy in translation, rotation, and vibration for H−H, H−D, D−H, and D−D reactions.

University College London, we performed our calculations using the DDPHP (doubly distributed parallel $\hat{H}\Psi$) method, recently developed by one of us.[54] The key idea behind this algorithm is to distribute the entire wave packet *twice*, so that each processor in the calculation contains two *different* slices of the wave packet. This means that no communication between the processors is required for all computations. The wave packet only needs to be resynchronized after each $\mathbf{H}q$ iteration. The result is that the percentage of the wave packet that has to be transferred in each iteration *decreases* with an increasing number of processors. This is in contrast to an algorithm in which the wave packet is only distributed once, because in that case the percentage of the wave packet to be transferred in each iteration actually *increases* with the increasing number of processors. The efficient communication characteristics of the DDPHP algorithm combined with an efficient computational layout means that the algorithm scales linearly with an increasing number of processors.[54] Use of the DDPHP algorithm greatly reduced the turnaround time for our calculations.

4. Results

In this section we first discuss the results of our 2D calculations. Subsequently, we will discuss the results for the 3D calculations. In the discussion of our results we use the following notation: A−B denotes a calculation with atom B colliding with A-on-graphite or in other words A(ad) + B(g) → AB(g), where A and B are H or D.

4.1. 2D Results. The 2D reaction probabilities are given in Figure 1. The total energy range that can be described correctly extends far beyond an initial translational energy of 2300 K to an initial translational energy of approximately 20 000 K. We only plot the region up to 2300 K to facilitate comparison with our earlier calculations and because it is the most relevant region for astrophysics. Note that this large energy range is a direct consequence of our decision to use two wave packets for the 2D calculations, a broad, low-energy wave packet and a narrow high-energy wave packet. All four isotope calculations have also been calculated with a time-independent method, as was done in ref 1. This allows us to get an idea of the lower energy limit for which our calculations still describe the physics of the reaction correctly. We find excellent agreement with the time-independent results. From that agreement we conclude that our calculations are definitely converged for energies down to 100 K.

All calculations shown in Figure 1 are converged apart from the quick oscillations in the D−H panel at just above 2000 K, which we will discuss later. The propagation times for the four different mass combinations vary from 3.137 and 4.821 ps for D−D and H−D, respectively, to 7.269 ps for H−H and 24.13 ps for D−H. The sharp oscillations in the D−H figure at just above 2000 K are most likely caused by the fact that at that energy the incoming hydrogen atom has just enough energy to excite the adsorbed deuterium atom to its first excited state for which 2025 K is needed. The result for a nonreactive collision is subsequently that the scattered hydrogen atom does not have enough energy to escape the system and will form a very long-lived complex with the adsorbed deuterium until reaction or de-excitation has occurred. A similar oscillatory pattern can be

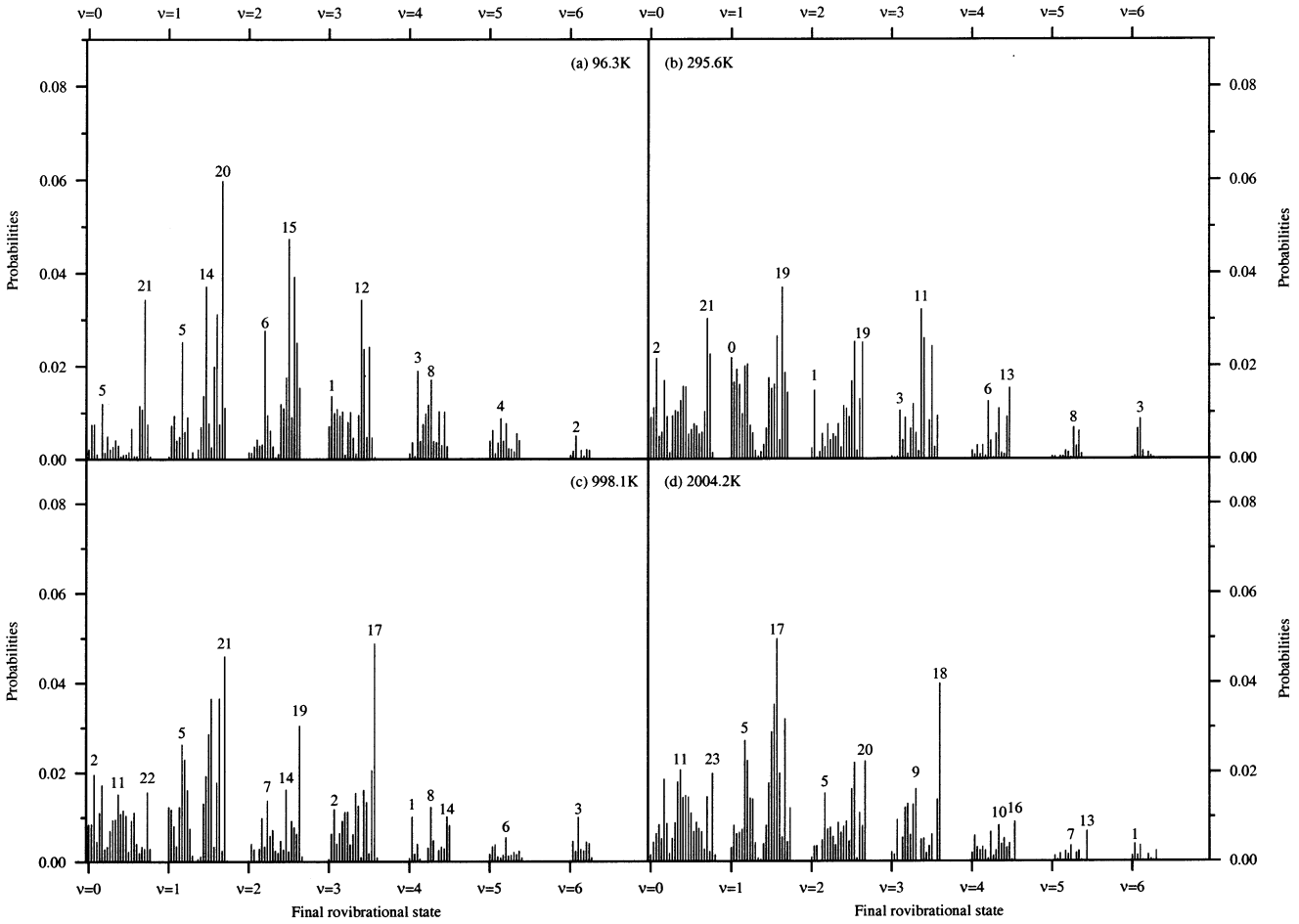

Figure 6. 3D state-resolved reaction probabilities for the H−D reaction at initial translational energies of 96.3, 295.6, 998.1, and 2004.2 K. Labels indicate the rotational quantum number of final rovibrational state.

TABLE 1: Resonance Energies and Lifetimes from the 2D Reaction Probabilities for the H−H, H−D, and D−H Reactions

reaction	resonance energy (K)	resonance lifetime (fs)
H−H	1177.0	51.2
H−D	653.9	62.6
	1402.4	36.9
	1934.1	50.5
D−H	936.5	98.6
	1244.4	102.3
	1571.4	275.9
	1909.0	302.1

found in the H−H and H−D total reaction probabilities around 2800 K (not pictured) where the incoming hydrogen/deuterium excites the adsorbed hydrogen to its first excited state, which lies 2801 K above the ground state. No such feature is found in the D−D total reaction probabilities, however.

Not only from the differences in total propagation time but also from the differences between the panels in Figure 1, it is clear that changing the mass combination in the calculations leads to a significant change in the dynamics. Nowhere is this more clear than when comparing the H−D and D−H results. Despite the fact that in both cases the same molecule (HD) is formed, the total reaction probabilities and state-resolved reaction probabilities are completely different. For the total reaction probabilities we find for H−D only very broad resonances, whereas for D−H they are much sharper.

A number of observations can be made regarding the state-resolved reaction probabilities. First, H−D is formed vibrationally hotter than D−H, because the maximum probability is for $\nu = 5$ in the former case versus $\nu = 4$ in the latter. Second, the behavior of the reaction probabilities as a function of initial translational energy across the resonances in the total reaction probability is completely different. For H−D, we see for example a steady increase in $\nu = 6$ across the first resonance coupled to a decrease in $\nu = 5$. This trend is reversed after the resonance, where an increase in $\nu = 5$ is coupled to a decrease in $\nu = 6$. For the D−H calculations, the situation is different. Here, e.g., for the first resonance, we also see a sharp increase in the $\nu = 6$ reaction probability coupled with decreases in all other reaction probabilities. However, in contrast to the $\nu = 6$ reaction probability for the H−D reaction here the $\nu = 6$ reaction probability peaks at the minimum in the reaction probability. Note that this is similar to the resonance feature in the H−H state-resolved reaction probability at approximately 1200 K, which is accompanied by a tiny dip in the reaction probability.

For each of the resonances in Figure 1 that can be considered to be resolved, we calculated the resonance lifetime using eq 3. The lifetimes are given in Figure 1. Together with the resonance energies, they are given in Table 1. Initially, one would think that the resonance structure for the H−D reaction can be expected, because this reaction geometry is a classic example of the heavy−light−heavy reaction. Many examples of such resonances have been found in 2D (collinear) calculations on gas-phase reactions. Most research on these systems was done on symmetric systems, such as, e.g., Cl + HCl,[73,74] I + HI,[75,76] or F + HF,[77,78] Asymmetric systems such as, e.g., Cl + HBr[75] have been studied as well (this list is by no means exhaustive; see, e.g., also refs 79 and 80 and references therein).

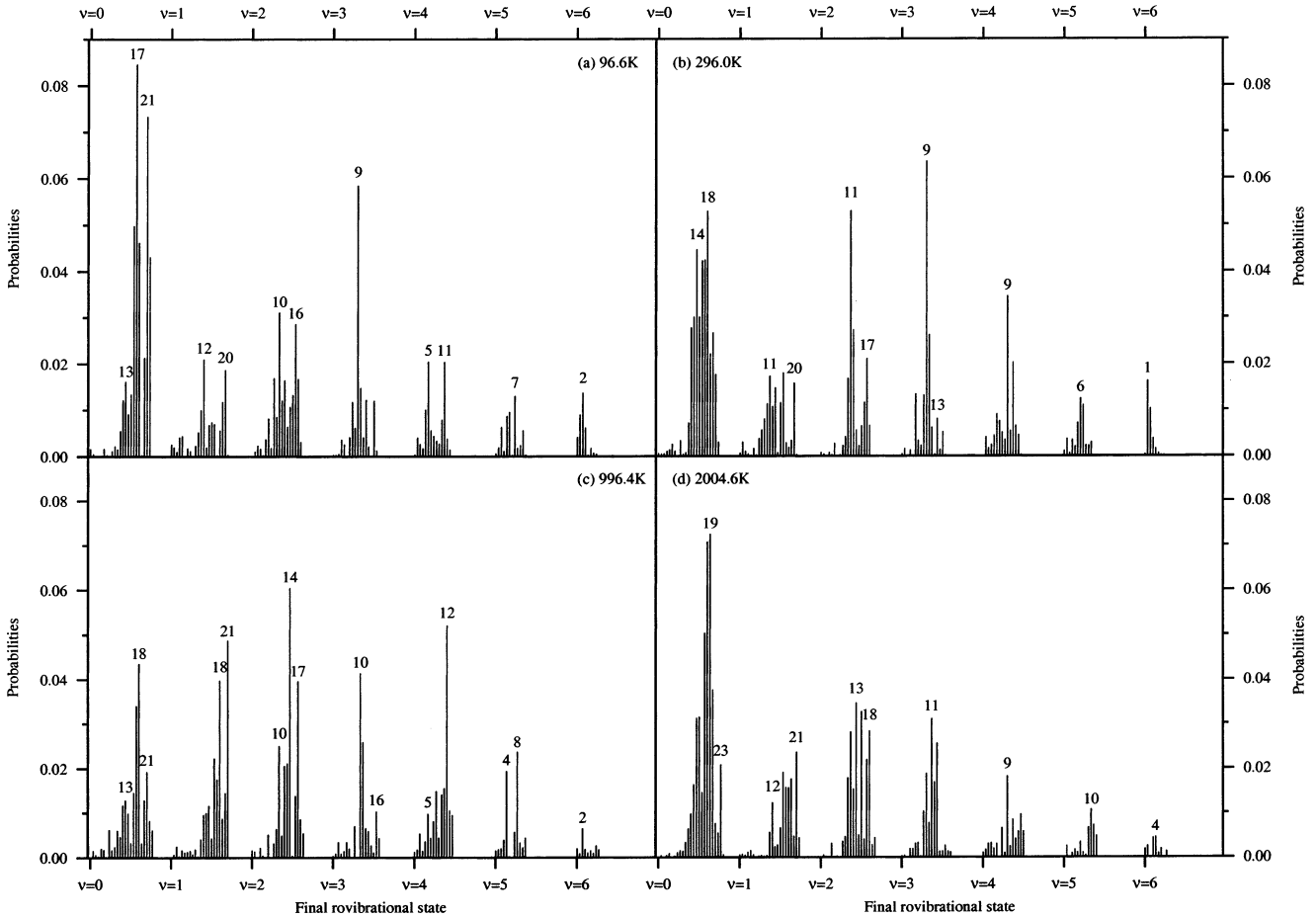

Figure 7. 3D state-resolved reaction probabilities for the D−H reaction at initial translational energies of 96.6, 296.0, 996.4, and 2004.6 K. Labels indicate rotational quantum number of final rovibrational state.

For a symmetric system these resonances occur with a spacing of approximately one vibrational quantum of the LH molecule. However, for our calculations the spacing between the resonance energies is much less than the H−graphite vibrational spacing, which is 2801 K for the first excited state and also much less than, e.g., the energy difference between the $\nu = 5$ and $\nu = 6$ states of H−D, which is 3886 K. Therefore, it must be due to vibrations of the HD molecule on the surface. To investigate this further, we have looked at the vibrational adiabatic levels of this system. These levels are calculated in the time-independent (TI) calculations we used to calibrate our time-dependent (TD) calculations and are therefore readily available. They are plotted for each of the mass combinations as a function of the hyperradius $\rho = \sqrt{S^2+s^2}$ in Figure 2, where S and s are the mass-weighted analogues of R and r, respectively. The state that is followed in the TI calculations is the solid red line indicated by the arrow (for more information on these types of calculations see, e.g., ref 2). For each of the mass combinations the vibrational adiabats contain local minima (some even show two!), which indicates the possibility of resonances. However, the precise differences in resonance lifetimes or the spacing between the resonances are most likely caused by subtle differences in the vibrational adiabats. They cannot be characterized so easily by a qualitative examination of the vibrational adiabats. Instead, this would require the calculation of the TI wave functions at the resonance energies, which falls outside the scope of the present work.

In Figure 3 we show the average final kinetic energy as a percentage of the total amount of energy in the system as a function of the initial translational energy. Here, it becomes clear that HD formed in the H−D reaction is indeed vibrationally hotter than the DH formed in the D−H reaction. It is also interesting for H−D that, despite the resonance structure in the total reaction probability and the sharp changes in the state-resolved reaction probability, the percentage average final translational energy is still more or less constant. This is in contrast to the H−H results and the D−H results, where the resonance structure in the state-resolved reaction probabilities from Figure 1 is more or less retained in the curves in Figure 3. This is another indication of the different resonance characteristics of the H−D reaction with respect to the D−H and H−H reactions.

4.2. 3D Results. The total 3D reaction probabilities are given in Figure 4. As mentioned before, these were generated using a high-speed, narrow wave packet. For the D−D system we were able to split the calculation into two parts corresponding to even and odd rotational states, like we did for H_2 in ref 1. The calculations show that there is almost no difference in the reaction probability between the formation of ortho-D_2 (even j) and the formation of para-D_2 (odd j). We did not include the nuclear spin of the atoms in our calculations. Thus, for all other reaction probabilities reported here, we simply averaged the ortho and para results.[81] Recent model calculations by Takahashi[82] suggest that H_2 on graphite will be formed in the "normal" 3:1 ortho:para ratio, which suggests also that D_2 should be formed in a 2:1 ortho:para ratio. There are no experimental measurements of the ortho:para ratio for H_2 or D_2 formed in a surface-catalyzed reaction.

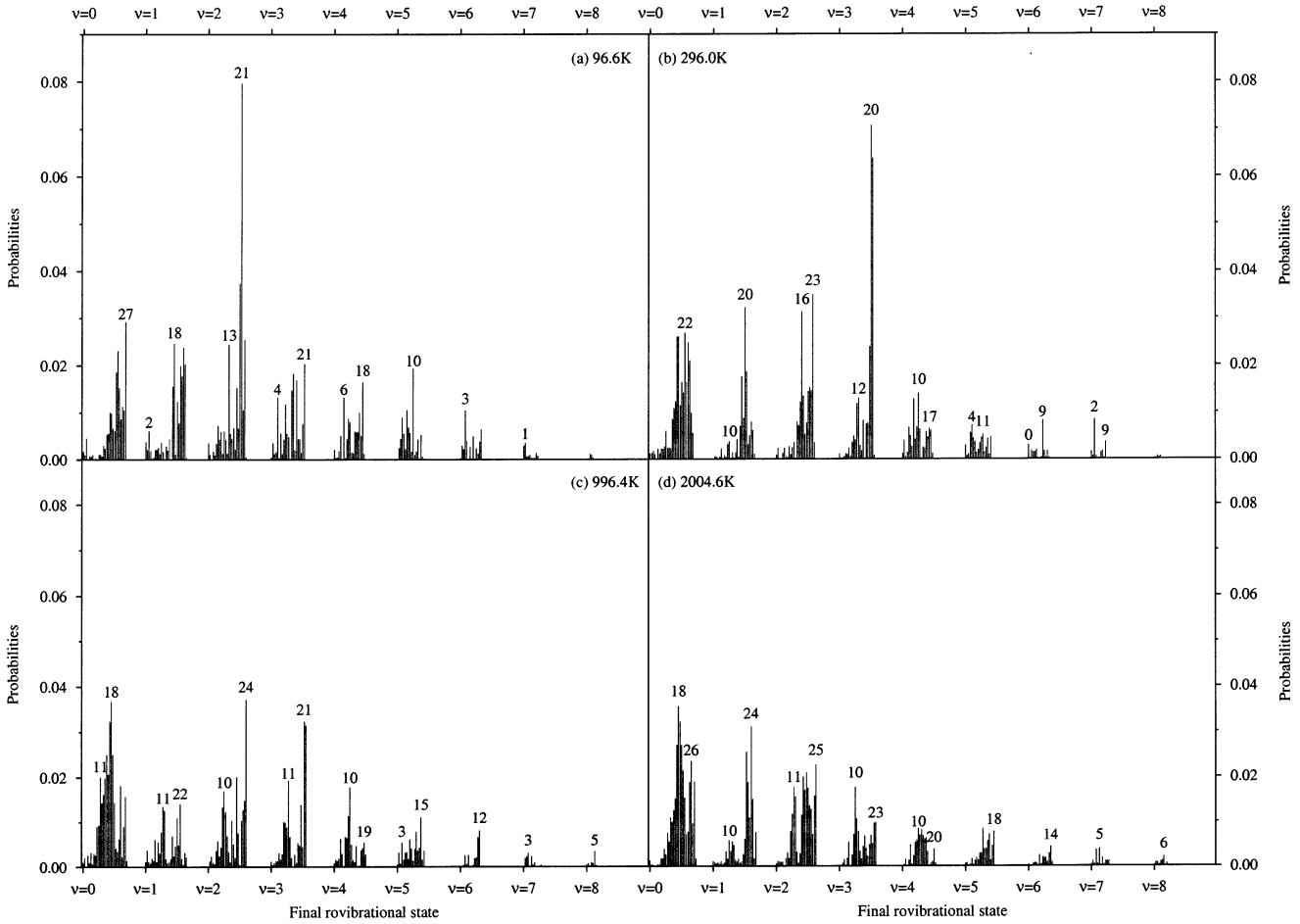

Figure 8. 3D state-resolved reaction probabilities for the D−D reaction at initial translational energies of 96.6, 296.0, 996.4, and 2004.6 K. Labels indicate rotational quantum number of final rovibrational state.

TABLE 2: Resonance Energies and Lifetimes from the 3D Reaction Probabilities for the H−D Reaction

resonance energy (K)	resonance lifetime (fs)
241	60.5
607	36.3
1240	30.4
1702	64
2053	21

From the total reaction probabilities in Figure 4 it is clear that the clean resonances from the 2D calculations are gone. We can still see some resonance structure. This is most clear for the H−D reaction, which is the heavy−light−heavy (HLH) reaction. If we ignore the substructure of the resonances, we can fit them to eq 3 to get the lifetimes. These are given in Table 2. The table clearly shows that that the resonances lie at different initial translational energies than in the 2D calculations. The lifetimes are of the same order of magnitude as in the 2D calculations. Such HLH reactions have been extensively studied in gas-phase reactions (see, e.g., refs 83−87). In gas-phase reactions the spacing of the oscillations is of the order of the spacing of the rotational levels of one of the constituent HL molecules. The oscillations are caused by a hindered rotation of the HL molecule in the HLH complex and do not involve rapid transfer of the light atom between the heavy atoms as in the 2D case. As a result, similar oscillations can also be found in nonreactive systems, like Ar−HBr.[84] In our calculations the spacing between the resonances is not similar to the rotational spacing in the resulting HD molecule. However, we still think that a similar explanation possibly holds here as well with a restricted bending motion of the HD molecule on the graphite surface taking the role of the hindered rotation from the gas phase.

We also investigated how the total energy available to the reactants is, on average, distributed between rotational, vibrational, and translational energy, where the partition between rotational energy and vibrational energy is done by assuming that the energy difference between the v, $j = 0$ state and the v, j state is solely rotational energy and that the energy difference between the $v = 0$, $j = 0$ state and the v, $j = 0$ state is purely vibrational energy. An alternative way of investigating this would have been to look at the average j and v quantum numbers.[32,34] However, that would have made comparison between the mass combinations impossible, because of different rovibrational energy spectra. For each of the four mass combinations, the fraction of the total available energy in each of the three types of energy together with the total reaction probability is given in Figure 5. For the H−H reaction and especially for the H−D reaction we find a correlation between maxima in the rotational energy fraction and maxima in the reaction probability. For the D−D reaction the situation is somewhat more complex. Here, we find correlation between the rotational energy fraction and the reaction probability at low initial translational energies. However, at high energies we find almost perfect correlation between the vibrational energy fraction and the reaction probability. The D−H reactive system is completely different from the other mass combinations. Here, at high energy we find correlation between the rotational energy fraction and the reaction probability, whereas at low energy there

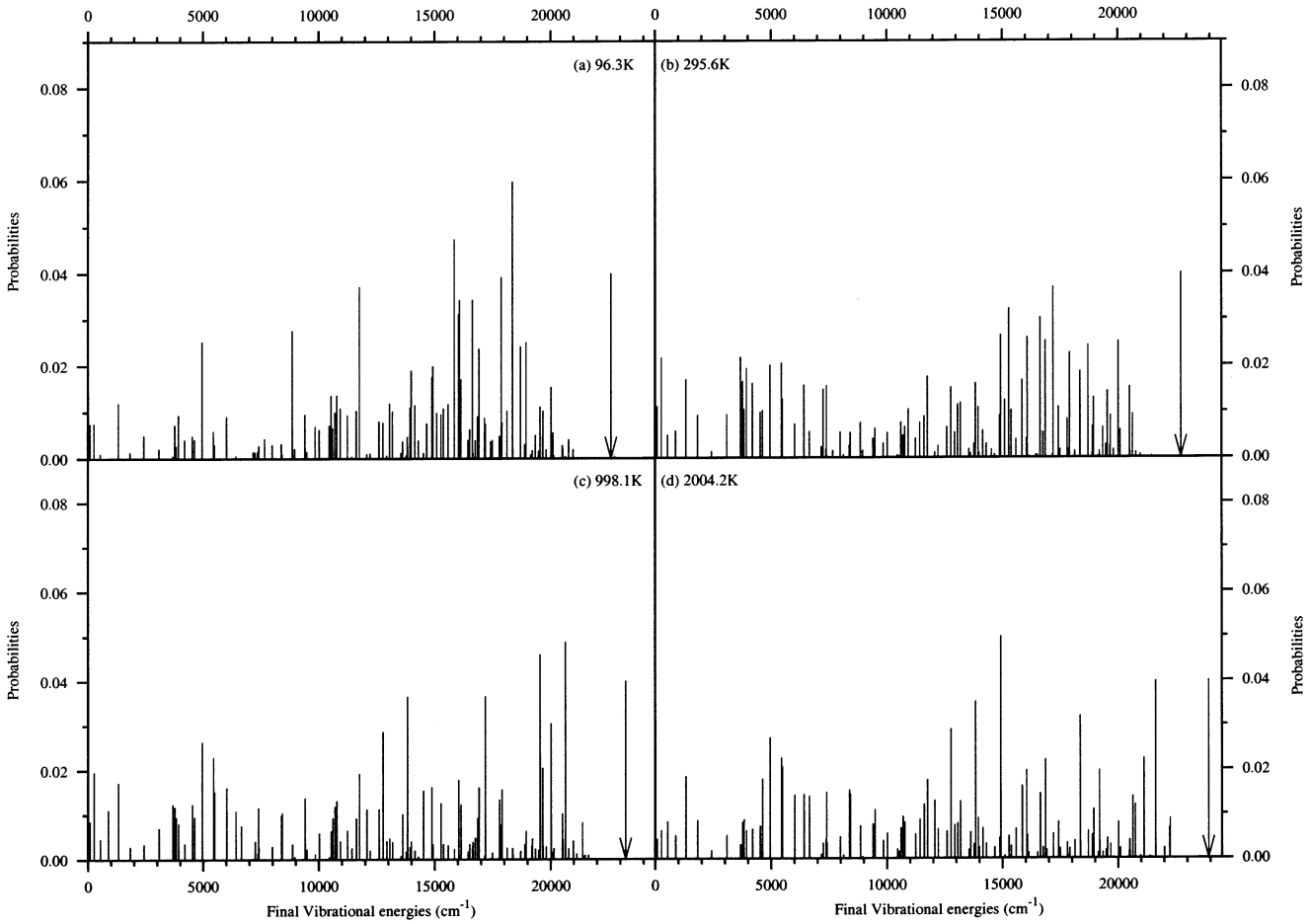

Figure 9. 3D state-resolved reaction probabilities as a function of final rovibrational energy for the H−D reaction at initial translational energies of 96.3, 295.6, 998.1, and 2004.2 K. Arrow indicates maximum available energy.

is no correlation at all. Here, the rotational energy fraction has a maximum after the reaction probability, where the vibrational energy fraction has a maximum before the reaction probability. In general, we find that for all mass combinations (apart from D_2) at almost all energies maxima in the average vibrational energy correspond to minima in the reaction probability. The reasons for these correlations cannot be determined from our calculations. Further elucidation therefore will require calculating TI wave functions at the resonance energies.

In the 2D calculations, the H−D reaction shows a lower translational energy fraction than the other mass combinations. For the 3D calculations the situation is different. Here, the translational energy fraction is higher than the translational energy fraction for the D−D and D−H reactions and similar to the translational energy fraction for the H−H reaction. Changing the mass combinations mainly affects the rotational energy fraction, whereas the vibrational energy fraction is more or less independent of the mass combination, especially at high initial translational energies. In general, we can say that adsorbing H on the graphite leads to a lower rotational energy fraction than when D is adsorbed on the surface, especially at high initial translational energies.

In Figures 6−8 we have plotted the normalized state resolved reaction probabilities for the H−D, D−H, and D−D reactions for four different initial translational energies, ∼96, ∼296, ∼1000, ∼2000 K (note that the energies differ slightly between different mass combinations). Interestingly, the maximum rovibrational state occupied for each of the mass combinations has approximately the same energy in each case (approximately 20 000 cm^{-1} for $T \approx 96$ K). Each mass combination has states that are significantly more populated than the neighboring states. The population in each of these states is highly dependent on the initial translational energy. For example, for the H−D reaction the ($v = 1$, $j = 20$) and ($v = 2$, $j = 15$), which are very prominent at 96 K are almost completely gone at 296 K. At 2004 K the most prominent states are ($v = 1$, $j = 17$) and ($v = 3$, $j = 18$). Similar observations can be made for the D−H and D−D reactions. On the other hand some rovibrational levels appear to be suppressed with respect to their neighbors, e.g., the ($v = 0$, $j = 19$), ($v = 1$, $j = 17$), ($v = 3$, $j = 5$), and ($v = 5$, $j = 6$) rovibrational states for DH at 97 K.

Inspection of the energy spectrum for each of the reactions correlated with the reaction probabilities shows that there are clusters of states, some of which are enhanced and some of which are suppressed. We have listed a characteristic example for each of the H−D, D−H, and D−D reactions at the lowest translational energy in Table 3. In this table we have indicated the vibrational and rotational quantum numbers, the rovibrational energy and whether the state is enhanced (+) or suppressed (−) with respect to its neighbors. ± means that no definite assignment can be made. For each of the mass combinations the spread in the asymptotic rovibrational energies is approximately 300 cm^{-1}. As is clear from the table, there appears to be a correlation between the increased intensity in some states and the decreased intensity in other states. It is also clear when checking different energies in Figures 6−8 that this correlation is dependent on the initial translational energy. For example, for the D−H reaction at $T = 296$ K the ($v = 1$, $j = 17$) state is enhanced, whereas the ($v = 3$, $j = 10$) and ($v = 2$, $j = 14$) states, which lie close to this state are suppressed. No such

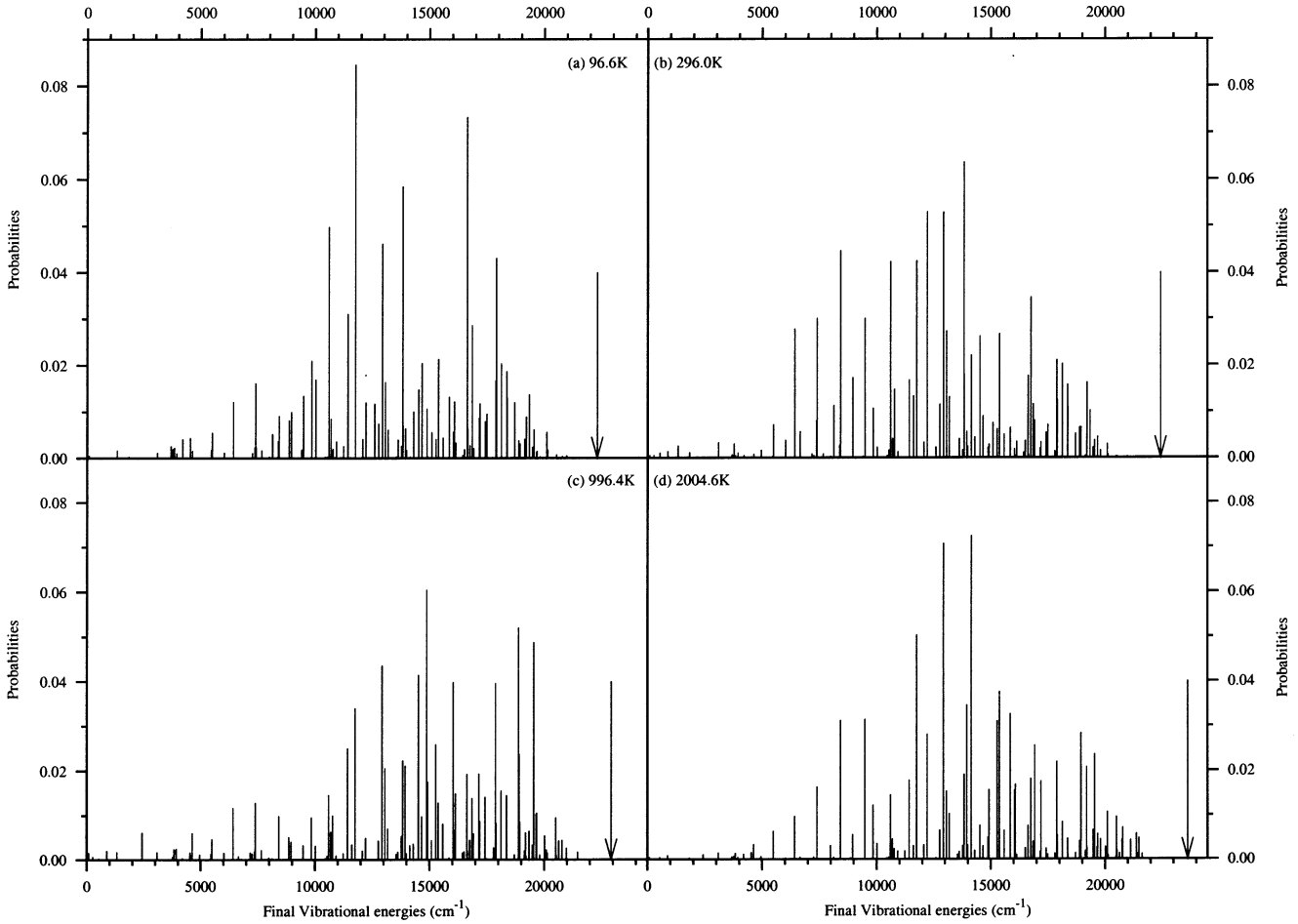

Figure 10. 3D state-resolved reaction probabilities as a function of final rovibrational energy for the D−H reaction at initial translational energies of 96.6, 296.0, 996.4, and 2004.6 K. Arrow indicates maximum available energy.

TABLE 3: Rovibrational Energies of States, Which Are Enhanced or Suppressed in the 3D Reaction Probability at 96 K for the H−D, D−H, and D−D Reactions

reaction	state	rotational energy (cm^{-1})	change
H−D	$v = 0, j = 17$	11749.8	−
	$v = 1, j = 14$	11751.3	+
	$v = 2, j = 10$	11427.0	−
	$v = 3, j = 5$	11618.3	±
D−H	$v = 0, j = 19$	14140.6	−
	$v = 2, j = 13$	13946.3	−
	$v = 3, j = 9$	13822.3	+
	$v = 4, j = 3$	13993.8	−
D−D	$v = 0, j = 26$	16883.7	−
	$v = 2, j = 21$	16963.8	+
	$v = 3, j = 18$	16870.5	±
	$v = 4, j = 15$	17058.4	±
	$v = 5, j = 11$	17009.5	
	$v = 6, j = 5$	16964.3	

correlation can be seen for this initial energy between the states listed in Table 3. Also, it is clear that the states showing a correlation for the H−D reaction do not show any correlation for the D−H reaction. Possible explanations for this correlation between product molecule rovibrational states include restricted bend states on the graphite surface having significant overlap with more than one asymptotic state or high Δj transitions in the exit channel.

The possibility of resonant high Δj transitions in the exit channel is interesting in itself. If these transitions are also probable in collision with, e.g., other H_2 molecules, then that might mean that the highly rotationally excited H_2 molecules that are predicted in our calculations will not be found in the interstellar medium, because they will have de-excited before they can be detected. We are currently investigating this de-excitation path further.[88]

In Figures 9−11 we plotted the normalized state selected reaction probability as a function of the final rovibrational energy at identical initial translational energies as in Figures 6−8. It is clear from each of the figures that the minimum amount of translational energy of the products is approximately 2000 cm^{-1} or about 10% of the total available energy. A similar conclusion was drawn for the H−H calculations in paper I. When the three figures are compared with Figure 8 in paper I, we find that for the D−H reaction the low rovibrational states are much less populated than, e.g., for the H−D reaction, with the H−H and D−D reactions lying between those two extremes, but more like the D−H reaction than the H−D reaction. We think that this is another manifestation of the fact that for the H−D reaction we are dealing with a heavy−light−heavy system, although this has not been mentioned before in the literature. A more definite answer to this would be provided by the calculation and characterization of all states in the interaction region.

There are no other calculations to compare our results with. Moreover, there is only one set of experiments on the formation of HD.[47−49] These experiments were setup with two atom sources, one in which H atoms were formed by dissociating H_2 and one in which D atoms were formed by dissociating D_2. The dissociation of H_2 or D_2 is not complete. However, HD can only be formed on the surface, which means that this does not have to be taken into account. The formation rates for HD

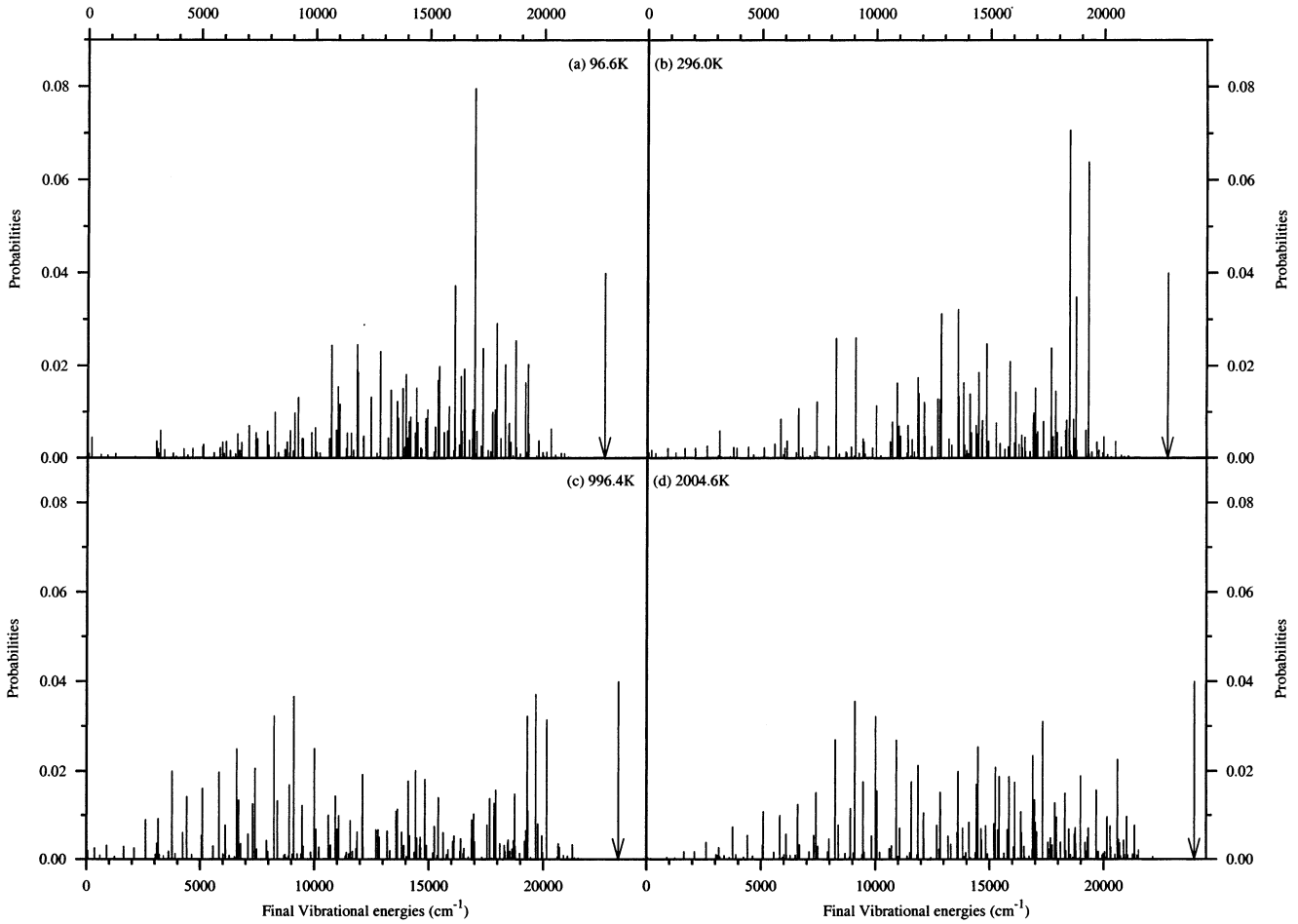

Figure 11. 3D state-resolved reaction probabilities as a function of final rovibrational energy for the D−D reaction at initial translational energies of 96.6, 296.0, 996.4, and 2004.6 K. Arrow indicates maximum available energy.

were subsequently used to predict rates for the formation of H_2 in the interstellar medium,[47,89] neglecting any isotope effects in the formation of H_2 or its isotopomers. However, our calculations suggest that isotope effects in this reaction will be large. This means that caution is needed in using the results for the formation of HD in predicting rates for the formation of H_2.

Unfortunately, these temperature-programmed desorption experiments did not yield any state-resolved results, making a detailed comparison with our calculations impossible. Moreover, they were performed at very low coverages of H and D on the graphite surface (<1%). For these low coverages the Eley−Rideal mechanism is not expected to be important. However, they did conclude that the H atoms did not move across the surface, making it possible that at higher coverages the Eley−Rideal reaction mechanism becomes the dominant reaction mechanism. Thus, we are currently developing a new potential that incorporates a much higher coverage of H/D on the graphite than the calculations on which the current potential is based. In the case of a full monolayer of H/D on the graphite surface we can also expect that cooperative effects within this monolayer will be important. We will therefore attempt to incorporate this in our calculations.[90]

5. Conclusions

We have performed both 2D and 3D calculations on H reacting with D adsorbed on graphite(0001), D reacting with H adsorbed on graphite(0001), and D reacting with D adsorbed on graphite(0001), leading to the formation of HD, DH, and D_2, respectively. These calculations were performed to investigate possible mass effects in the formation of H_2 on graphite, an important process in the formation of H_2 in the interstellar medium, which was reported on in previous papers.[1,2] For the current calculations, we used similar approximations as for our calculations on the formation of H_2. Thus, we neglected the corrugation of the surface and kept the surface fixed. The potential used was that developed in ref 1. As is the case with all potentials developed for this system, the potential can only be expected to have qualitative accuracy. A more accurate potential combined with a more rigorous description of the dynamics will obviously change our results to some extent.

The 2D calculations show remarkable differences between the different mass combinations. Moreover, we find evidence for resonances in the formation of H_2, DH, and HD. The resonances are associated with states of the adsorbed HD, DH, and HH molecules on graphite. The behavior of the resonances as a function of initial energy and the fraction final vibrational energy of the total energy suggest that the reaction of D with adsorbed H (i.e., the formation of H−D in a heavy-light-heavy reaction geometry) has a reaction mechanism different from the reaction of H with adsorbed D (the formation of D−H) and the reaction of H with adsorbed H. No resonances were found in the reaction of D with adsorbed D. In all cases we find vibrationally highly excited products.

Most of the resonance structure in the 2D total reaction probability has disappeared in the 3D total reaction probabilities. Also, we find much less vibrational excitation, as in the 2D case, although the products are highly rotationally excited. We

can still identify some resonance structure, particularly in the H−D reaction. As with the 3D heavy−light−heavy (HLH) reactions in the gas phase, we attribute this to restricted bend states. The main difference with the gas phase is that in a gas−surface reaction the restricted bend state is of the molecule on the surface and not of the one LH molecule in the HLH complex. We find clear correlations between increases in the rotational energy fraction of the total energy and increases in the total reaction probability. We also find energy-dependent correlations between final rovibrational states, which are clearly enhanced with respect to other states and other final rovibrational states, which are clearly suppressed. Two possible explanations are given. We also find that in the formation of H−D no low-energy rovibrational states are occupied compared to the situation in the formation of D−H. This is tentatively attributed to the fact that the H−D reaction is a heavy−light−heavy reaction, whereas the formation of D−H is not.

Concluding, we can say that HD and D_2, like H_2, will be formed rovibrationally excited and translationally hot. This finding could have important implications for the interstellar medium, because initial vibrational excitation and high translational energy can significantly enhance the reactivity of H_2 and its isotopomers. We also find strong isotope effects, which has consequences for the use of experiments on HD to predict the formation rates of H_2.

Acknowledgment. The research was funded by the Particle Physics and Astronomy Research Council, the Engineering and Physical Sciences Research Council, and the Leverhulme Trust. We thank the members of the Centre for Cosmic Chemistry and Physics at University College London for helpful discussions.

References and Notes

(1) Meijer, A. J. H. M.; Farebrother, A. J.; Clary, D. C.; Fisher, A. J. *J. Phys. Chem. A* **2001**, *105*, 2173.
(2) Farebrother, A. J.; Meijer, A. J. H. M.; Clary, D. C.; Fisher, A. J. *Chem. Phys. Lett.* **2000**, *319*, 303.
(3) Rettner, C. T.; Michelsen, H. A.; Auerbach, D. J. *J. Chem. Phys.* **1995**, *102*, 4625.
(4) Rettner, C. T.; Auerbach, D. J.; Tully, J. C.; Kleyn, A. W. *J. Phys. Chem.* **1996**, *100*, 13021.
(5) Hou, H.; Goulding, S. J.; Rettner, C. T.; Wodtke, A. M.; Auerbach, D. J. *Science* **1997**, *277*, 80.
(6) Hodgson, A.; Moryl, J.; Traversaro, P.; Zhao, H. *Nature* **1992**, *356*, 501.
(7) Darling, G. R.; Holloway, S. *Faraday Discuss.* **1998**, *110*, 253.
(8) Dai, J.; Light, J. C. *J. Chem. Phys.* **1998**, *108*, 7816.
(9) Kroes, G.-J.; Baerends, E.-J.; Mowrey, R. C. *Phys. Rev. Lett.* **1997**, *78*, 3583.
(10) Kroes, G.-J. *Prog. Surf. Sci.* **1999**, *60*, 1 and references therein.
(11) Kroes, G.-J.; Baerends, E.-J.; Mowrey, R. C. *J. Chem. Phys.* **1997**, *107*, 3309.
(12) Munn, N. S.; Clary, D. C. *J. Chem. Phys.* **1996**, *105*, 5258.
(13) Kay, M.; Darling, G. R.; Holloway, S. *J. Chem. Phys.* **1998**, *108*, 4614.
(14) Gross, A.; Wilke, S.; Scheffler, M. *Phys. Rev. Lett.* **1995**, *75*, 2718.
(15) Eley, D. D.; Rideal, E. K. *Nature* **1940**, *146*, 401.
(16) Kolovos-Vellianitis, D.; Kammler, T.; Küppers, J. *Surf. Sci.* **2000**, *454*−*456*, 316.
(17) Okada, M.; Moritani, K.; Nakamura, M.; Kasai, T.; Murata, Y. *Chem. Phys. Lett.* **2000**, *323*, 586.
(18) Böttcher, A.; Niehus, H.; Schwegmann, S.; Over, H.; Ertl, G. *J. Phys. Chem. B* **1997**, *101*, 11185.
(19) Böttcher, A.; Niehus, H. *Phys. Rev. B* **1999**, *60*, 14396.
(20) Burch, R.; Shestov, A. A.; Sullivan, J. A. *J. Catal.* **1999**, *188*, 69.
(21) Weinberg, W. H. *Acc. Chem. Res.* **1996**, *29*, 479.
(22) Mitchell, W. J.; Xie, J.; Jachimowski, T. A.; Weinberg, W. H. *J. Am. Chem. Soc.* **1995**, *117*, 2606.
(23) Xie, J.; Mitchell, W. J.; Lyons, K. J.; Weinberg, W. H. *J. Chem. Phys.* **1994**, *101*, 9195.
(24) Kalyanaraman, C.; Lemoine, D.; Jackson, B. *Phys. Chem. Chem. Phys.* **1999**, *1*, 1351.
(25) Persson, M.; Jackson, B. *J. Chem. Phys.* **1995**, *102*, 1078.
(26) Jackson, B.; Persson, M. *J. Chem. Phys.* **1995**, *103*, 6257.
(27) Caratzoulas, S.; Jackson, B.; Persson, M. *J. Chem. Phys.* **1997**, *107*, 6420.
(28) Shalashilin, D. V.; Jackson, B. *J. Chem. Phys.* **1998**, *109*, 2856.
(29) Shalashilin, D. V.; Jackson, B.; Persson, M. *J. Chem. Phys.* **1999**, *110*, 11038.
(30) Kratzer, P. *J. Chem. Phys.* **1997**, *106*, 6752.
(31) Jackson, B.; Lemoine, D. *J. Chem. Phys.* **2001**, *114*, 474.
(32) Sha, X.; Jackson, B. *Surf. Sci.* **2002**, *496*, 318.
(33) Parneix, P.; Bréchignac, P. *Astron. Astrophys.* **1998**, *334*, 363.
(34) Rutigliano, M.; Cacciatore, M.; Billing, G. D. *Chem. Phys. Lett.* **2001**, *340*, 13.
(35) Ree, J.; Kim, Y. H.; Shin, H. K. *Chem. Phys. Lett.* **2002**, *353*, 368.
(36) van der Hulst, H. C. *Rec. Astron. Obs.* **1949**, *XI(II)*.
(37) Gould, R. J.; Salpeter, E. E. *Astrophys. J.* **1963**, *138*, 393.
(38) Hollenbach, D.; Salpeter, E. E. *Astrophys. J.* **1971**, *163*, 155.
(39) Williams, D. A.; Herbst, E. *Surf. Sci.* **2002**, *500*, 823.
(40) Hoppe, P.; Zinner, E. *J. Geophys. Res. Space Res.* **2000**, *105*, 10371.
(41) Bernatowicz, T. J.; Cowsik, R.; Gibbons, P. C.; Lodders, K.; Fegley, B., Jr.; Amari, S.; Lewis, R. S. *Astrophys. J.* **1996**, *472*, 760.
(42) Messenger, S.; Amari, S.; Gao, X.; Walker, R. M.; Clemett, S. J.; Chillier, X. D. F.; Zare, R. N.; Lewis, R. S. *Astrophys. J.* **1998**, *502*, 284.
(43) Mathis, J. S.; Rumpl, W.; Nordsieck, K. H. *Astrophys. J.* **1977**, *217*, 425.
(44) Fitzpatrick, E. L.; Massa, D. *Astrophys. J. Suppl. Ser.* **1990**, *72*, 163.
(45) Li, A. G.; Greenberg, J. M. *Astron. Astrophys.* **1997**, *323*, 566.
(46) Papoular, R.; Conard, J.; Guillois, O.; Nenner, I.; Reynaud, C.; Rouzaud, J.-N. *Astron. Astrophys.* **1996**, *315*, 222.
(47) Katz, N.; Furman, I.; Biham, O.; Pirronello, V.; Vidali, G. *Astrophys. J.* **1999**, *522*, 305.
(48) Pirronello, V.; Liu, C.; Roser, J. E.; Vidali, G. *Astron. Astrophys* **1999**, *344*, 681.
(49) Pirronello, V.; Biham, O.; Manicó, G.; Rosen, J. E.; Vidali, G. In *Molecular Hydrogen in Space*; Combes, F., Pineau des Forêts, G., Eds.; Cambridge University Press: Cambridge, U.K., 2000; p 71.
(50) Ghio, E.; Mattera, L.; Salvo, C.; Tommasini, F.; Valbusa, U. *J. Chem. Phys.* **1980**, *73*, 556.
(51) Sidis, V.; Jeloaica, L.; Borisov, A. G.; Deutscher, S. A. In *Molecular Hydrogen in space*; Combes, F., Pineau des Forêts, G., Eds.; Cambridge University Press: Cambridge, U.K., 2000; p 89.
(52) Sha, X.; Jackson, B.; Lemoine, D. *J. Chem. Phys.* **2002**, *116*, 7158.
(53) Jeloaica, L.; Sidis, V. *Chem. Phys. Lett.* **1999**, *300*, 157.
(54) Meijer, A. J. H. M. *Comput. Phys. Commun* **2001**, *141*, 330.
(55) Schwartz, C. *J. Math. Phys.* **1985**, *26*, 411.
(56) Groenenboom, G. C.; Colbert, D. T. *J. Chem. Phys.* **1993**, *99*, 9681.
(57) Note the error with the signs in refs 56 and 58.
(58) Groenenboom, G. C. Private communication, 1996.
(59) Light, J. C.; Hamilton, I. P.; Lill, J. V. *J. Chem. Phys.* **1985**, *82*, 1400.
(60) Choi, S. E.; Light, J. C. *J. Chem. Phys.* **1989**, *90*, 2593.
(61) Whitnell, R. M.; Light, J. C. *J. Chem. Phys.* **1989**, *89*, 3674.
(62) Webster, F.; Light, J. C. *J. Chem. Phys.* **1989**, *90*, 265.
(63) McCreery, J. H.; Wolken, G., Jr. *J. Chem. Phys.* **1975**, *63*, 2340.
(64) Gray, S. K.; Balint-Kurti, G. G. *J. Chem. Phys.* **1998**, *108*, 950.
(65) Meijer, A. J. H. M.; Goldfield, E. M.; Gray, S.; Balint-Kurti, G. G. *Chem. Phys. Lett.* **1998**, *293*, 270.
(66) Balint-Kurti, G. G.; Gonzales, A. I.; Gray, S. K.; Goldfield, E. M. *J. Chem. Soc., Faraday Discuss.* **1998**, *110*, 169.
(67) Gray, S. K.; Goldfield, E. M.; Schatz, G. C.; Balint-Kurti, G. G. *Phys. Chem. Chem. Phys.* **1999**, *1*, 1141.
(68) Gray, S. K.; Wozny, C. E. *J. Chem. Phys.* **1989**, *91*, 7671.
(69) Zhang, D. H.; Zhang, J. Z. H. *J. Chem. Phys.* **1994**, *101*, 3671.
(70) Meijer, A. J. H. M.; Goldfield, E. M. *J. Chem. Phys.* **1998**, *108*, 5404.
(71) Clary, D. C.; Schatz, G. C. *J. Chem. Phys.* **1993**, *99*, 4582.
(72) Clary, D. C.; Meijer, A. J. H. M. *J. Chem. Phys.* **2002**, *116*, 9829.
(73) Bondi, D. K.; Connor, J. N. L.; Manz, J.; Römelt, J. *Mol. Phys.* **1983**, *50*, 467.
(74) Shoemaker, C. L.; AbuSalbi, N.; Kouri, D. J. *J. Chem. Phys.* **1983**, *78*, 5389.
(75) Babamov, V. K.; Lopez, V.; Marcus, R. A. *J. Chem. Phys.* **1983**, *78*, 5621.
(76) Hiller, C.; Manz, J.; Miller, W. H.; Römelt, J. *J. Chem. Phys.* **1983**, *78*, 3850.
(77) Aquilanti, V.; Grossi, G.; Laganà, A. *Chem. Phys. Lett.* **1982**, *174*, 174.
(78) Aquilanti, V.; Cavalli, S.; Grossi, G.; Laganà, A. *J. Mol. Struct.* **1984**, *107*, 95.
(79) Römelt, J. In *The Theory of Chemical Reaction Dynamics*; Clary, D. C., Ed.; Kluwer Academic: Dordrecht, The Netherlands, 1986.

(80) Grayce, B. B.; Skodje, R. T.; Hutson, J. M. *J. Chem. Phys.* **1993**, *98*, 3929.
(81) Separate results for ortho-D_2 and para D_2 are available on request.
(82) Takahashi, J. *Astrophys. J.* **2001**, *561*, 254.
(83) Grayce, B. B.; Skodje, R. T. *J. Phys. Chem.* **1992**, *96*, 4134.
(84) Grayce, B. B.; Skodje, R. T.; Hutson, J. M. *J. Chem. Phys.* **1993**, *98*, 3929.
(85) Mil'nikov, G. V.; Tolstikhin, O. I.; Nobusada, K.; Nakamura, H. *Phys. Chem. Chem. Phys.* **1999**, *1*, 1159.
(86) Noli, C.; Connor, J. N. L.; Rougeau, N.; Rubach, C. *Phys. Chem. Chem. Phys.* **2001**, *3*, 3946.
(87) Skodje, R. T. *J. Chem. Phys.* **1991**, *95*, 7234.
(88) Pogrebnya, S. K.; Meijer, A. J. H. M.; Clary, D. C. Work in progress.
(89) Biham, O.; Furman, I.; Pirronello, V.; Vidali, G. *Astrophys. J.* **2001**, *553*, 595.
(90) Meijer, A. J. H. M.; Clary, D. C.; Fisher, A. J. Work in progress.